Influence of Acylation of a Peptide Corresponding to the Amino-Terminal Region of Endothelial Nitric Oxide Synthase on the Interaction with Model Membranes†

Belén Yélamos,‡ Fernando Roncal,§ Juan P. Albar,§ Ignacio Rodríguez-Crespo,‡ and Francisco Gavilanes*,‡

Departamento de Bioquímica y Biología Molecular, Facultad de Ciencias Químicas, Universidad Complutense, 28040 Madrid, Spain, and Departamento de Inmunología y Oncología, Centro Nacional de Biotecnología, CSIC, 28049 Madrid, Spain

Received July 27, 2005; Revised Manuscript Received December 5, 2005

ABSTRACT: Covalent attachment of fatty acids to proteins is a common form of protein modification which has been shown to influence both structure and interaction with membranes. Endothelial nitric oxide synthase (eNOS) is dually acylated by the fatty acids myristate and palmitate. We have synthesized four peptides corresponding to the first 28 amino acids of the N-terminal region of eNOS. Besides the nonacylated eNOS sequence, three additional peptides with different degrees of acylation have been obtained: myristoylated, doubly palmitoylated, and dually myristoylated and doubly palmitoylated. Acylation itself, myristic and/or palmitic, confers the peptide the ability to adopt extended conformations, indicated by the fact that the CD spectrum of all acylated peptides has a minimum at ∼215 nm characteristic of β-sheet structure. The nonacylated sequence interacts with model membranes composed of acidic phospholipids probably through ionic interactions with the polar headgroup of the phospholipids. However, the acylated peptides are able to insert deeply into the hydrophobic core of both neutral and acidic phospholipids, maintaining the spectral features of extended conformations. When DMPC vesicles containing cholesterol and sphingomyelin at 10% were used, the insertion of the triacylated peptide almost completely canceled the thermal transition, although the interaction of the other acylated peptides also reduced the transition amplitude but to a much lower extent and affected only the acyl chains in the fluid state.

Protein acylation by myristic and palmitic acid is a widely occurring process which is involved in membrane binding as well as in cellular signaling (*1*). Myristoylation is a cotranslational and irreversible process that adds a myristic acid through an amide bond on the N-terminal glycine residue of the protein within a specific consensus sequence. The enzyme responsible for myristoylation is the *N*-myristoyl transferase (NMT)[1] that catalyzes transfer of myristate from myristoyl-CoA to suitable peptide and protein substrates. To date, nearly 20 NMTs from fungal and mammalian sources have been identified (*2*−*4*). On the other hand, palmitoylation is a reversible and post-translational process. S-Acylation occurs on cysteine residues through a thioester linkage in a wide variety of sequence contexts (*5*). This attachment is more labile than the amide linkage and facilitates the interaction of the acylated protein with membranes (*6*). Recently, the molecular identity of protein acyltransferases that modify palmitoylated proteins has been discovered (*5*). Two yeast palmitoyl-acyl transferases for intracellular proteins have been identified, Erf2/Erf4 and Akr1, which palmitoylate Ras2 and yeast casein kinase 2, respectively (*7*, *8*). Erf2 and Akr1 share a common domain, the Asp-His-His-Cys (DHHC) domain, within a cysteine-rich domain. The finding that these unrelated proteins share a common protein domain that is essential for protein acyltransferase activity has led to the identification of a functional ortholog of the yeast Ras palmitoyltransferase, the DHHC9−GCP16 complex (*9*). Nevertheless, nonenzymatic palmitoylation in vitro has also been demonstrated as the palmitoylation of a myristoylated peptide with the N-terminal sequence of the $p62^{Yes}$ protein tyrosine kinase (*10*), the myristoylated Giα protein (*11*), the 25 kDa synaptosomal protein (SNAP-25) (*12*), and small peptides of the β_2-adrenergic receptor (*13*). By using artificial sequences, we have obtained data which support the nonenzymatic protein palmitoylation within mammalian cells (*14*).

The dually acylated endothelial nitric oxide synthase (eNOS) enzyme produces the endothelium-derived nitric oxide (•NO) which is an important signaling molecule involved in many biological processes such as the regulation of blood pressure, platelet aggregation, and the maintenance of the vascular tone in both veins and arteries. Diminished •NO production has been implicated in the pathogenesis of a variety of vascular disorders, including atherosclerosis and pulmonary hypertension (*15*−*17*). The synthesis of endothelium-derived •NO is a calcium- and calmodulin-dependent process. This enzyme is dually acylated by myristic acid on

† This work was supported by grants from the Dirección General de Investigación, Ministerio de Educación y Ciencia, Spain (BMC 2003-06631 and BMC 2003-05034).

* To whom correspondence should be addressed. Telephone: +34 913944266. Fax: +34 913944159. E-mail: pacog@bbm1.ucm.es.

‡ Universidad Complutense.

§ CSIC.

[1] Abbreviations: DMPC, dimyristoylphosphatidylcholine; DMPG, dimyristoylphosphatidylglycerol; DMSO, dimethyl sulfoxide; DPH, 1,6-diphenyl-1,3,5-hexatriene; eNOS, endothelial nitric oxide synthase; NMT, *N*-myristoyl transferase; •NO, nitric oxide; PC, egg phosphatidylcholine; PG, egg phosphatidylglycerol; TFE, trifluoroethanol; TMA-DPH, 1-[4-(trimethylammoniumphenyl)-6-phenyl]-1,3,5-hexatriene.

10.1021/bi0514865 CCC: $33.50
Published on Web 01/06/2006

the N-terminal glycine and by palmitic acid on two cysteine residues: Cys15 and Cys26 (*18*−*20*). Myristoylation of eNOS is required for the subcellular location (*20*, *21*), the efficient production of •NO (*22*), and the subsequent palmitoylation (*19*), but it does not seem that myristoylation of eNOS alone could be responsible for the association of eNOS with membranes (*23*). Both myristoylation and palmitoylation are required to target eNOS to specialized membrane microdomains named caveolae where it is associated with caveolin at low cellular calcium concentrations (*23*, *24*). The association of eNOS with caveolin leads to an inhibition of eNOS activity (*23*). The cellular stimulation with agonists that increase the intracellular concentration of Ca^{2+} promotes the binding of calmodulin to eNOS and relieves the inhibition of the eNOS enzyme by caveolin (*18*).

In this work, we have synthesized four peptides corresponding to the first 28 amino acids of eNOS with different degrees of acylation: nonacylated, singly myristoylated on the amino-terminal Gly, doubly palmitoylated on the two cysteine residues, and dually myristoylated and doubly palmitoylated peptides. At the carboxyl end, we have added a tryptophan residue to monitor the fluorescence properties of each peptide. Subsequently, we have studied the structural properties of these four peptides and their interaction with liposomes of a defined composition.

EXPERIMENTAL PROCEDURES

Materials. Egg phosphatidylcholine (PC), egg phosphatidylglycerol (PG), dimyristoylphosphatidylcholine (DMPC), dimyristoylphosphatidylglycerol (DMPG), cholesterol, and sphingomyelin were provided by Avanti Polar Lipids. 1,6-Diphenyl-1,3,5-hexatriene (DPH) and 1-[4-(trimethylammoniumphenyl)-6-phenyl]-1,3,5-hexatriene (TMA-DPH) were purchased from Molecular Probes. All other reagents were from Merck.

Synthesis of Peptides. Synthesis was carried out on an automated multiple-peptide synthesizer (AMS 422, Abimed) using a solid-phase procedure and a standard Fmoc chemistry in a base of 25 μmol. It was used an N-α-Fmoc-DMP resin [4-(2′,4′-dimethoxyphenyl-Fmoc-aminomethyl)phenoxy resin (Novabiochem)] with Fmoc-protected amino acids activated in situ with PyBop (benzotriazol-1-yl-oxi-tris-pyrrolidino-phosphonium hexafluorophosphate) in the presence of *N*-methylmorpholine and a 20% piperidine/dimethylformamide mixture for deprotection. The protecting side chain groups were as follows: Asn and Gln (Trt), Glu (OtBu), Ser (tBu), Lys and Trp (Boc), and Cys (Acm). Peptides were cleaved from the resin with 82.5% trifluoroacetic containing 5% phenol, 5% water, 5% thioanisole, and 2.5% ethanedithiol as scavengers (*25*), precipitated, and washed with cold methyl *tert*-butyl ether, water-extracted, lyophilized, and purified by reverse-phase HPLC using a SuperPac7 Pep-S C2/C18 column (Pharmacia). Two different systems were used to purify the peptides. The nonacylated and myristoylated peptides were dissolved in 5% acetonitrile in 0.1% trifluoroacetic acid (TFA), and a gradient of acetonitrile and 0.1% TFA from 5 to 60% over the course of 35 min and from 60 to 100% over the course of 5 min was employed to elute them at a flow rate of 1 mL/min. In the case of palmitoylated and dually acylated peptides, ethanol (60%, v/v) in 0.1% TFA served as the initial mobile phase, and peptides were eluted with a 5 to 100% linear gradient of propan-2-ol and 0.1% TFA, over the course of 35 min at 0.7 mL/min. The absorbance at 214 nm was monitored continuously, and relevant peaks were collected manually, pooled, and lyophilized. The purified peptides were characterized by amino acid analysis, performed on a Beckman 6300 amino acid analyzer, PAGE, HPLC, and fast atom bombardment mass spectrometry using a Bruker mod Reflex III mass spectrometer. Because of the low solubility of peptides in aqueous buffers, a 5−10 mg/mL stock solution of the peptide in trifluoroethanol (TFE) or dimethyl sulfoxide (DMSO) was used in the various assays described in this work and kept at −20 °C between uses. The final organic solvent concentration was always kept under 2% (v/v).

Acylation of Peptides. Myristoylation and palmitoylation of peptides were performed on the synthesis resin. The myristic acid was activated with dicyclohexylcarbodiimide that renders the asymmetric anhydride and added in excess to the peptide attached to the resin. This causes the formation of the amide bond. Once the peptide was myristoylated, it was cleaved from the resin. The palmitoylation was carried out according to the protocol of Beekman et al. (*26*). After the synthesis, the protected peptide resin was washed with dimethylformamide (DMF) and the side chains of cysteine residues were liberated with 0.1 M mercury acetate in DMF. After completion of the reaction, the resin was washed copiously with DMF. Then, the sulfhydryl groups were reduced with a β-mercaptoethanol/DMF mixture (9:1) for 3 h. Free SH groups were palmitoylated on the resin by coupling using 8 equiv of PyBop, 8 equiv of palmitic acid, and 16 equiv of diisopropylethylamide (DIEA) in DMF, for 16 h at 37 °C. Then, the peptide was cleaved from the resin.

Vesicle Preparation. In all cases, a lipid film was obtained by drying a chloroform solution of the lipid under a current of nitrogen; this film was kept under vacuum for 5 h. The phospholipid was resuspended at a concentration of 1 mg/mL in medium buffer [5 mM Tris (pH 7.0), 100 mM NaCl, 5 mM MES, 5 mM sodium citrate, and 1 mM EDTA] or 20 mM sodium phosphate buffer (pH 7.0) for 1 h at 37 °C and eventually vortexed. This suspension was sonicated in a bath sonicator (Branson 1200) and was subsequently subjected to at least 15 cycles of extrusion in a Liposofast-Basic apparatus (Avestin) with 100 nm polycarbonate filters (Avestin). A 0.14 mM final phospholipid concentration was used in all the experiments.

Circular Dichroism Measurements. Circular dichroism spectra were obtained on a Jasco J-715 spectropolarimeter using a 0.1 cm path length cuvette at 25 °C. The peptide concentration was 80 μM. The buffer used was 20 mM sodium phosphate (pH 7.0) or TFE. A minimum of four spectra were accumulated for each sample, and the contribution of the buffer was always subtracted. The resultant spectra were smoothed using J-715 Noise Reduction software. The values of mean residue molar ellipticity $[\Theta]_{MRW}$ were calculated on the basis of 100 as the average molecular mass per residue, and they are reported in terms of degrees per square centimeter per decimole. The spectra in the presence of lipid vesicles were recorded after incubation of 1 h at 37 °C. To minimize the effect of light scattering on the shape and magnitude of the spectrum, lipid/peptide mixtures were sonicated before the spectra were recorded.

Table 1: Synthesized Peptides Corresponding to the N-Terminal Sequence of eNOS[a]

peptide	sequence
eNOS	GNLKSVGQEPGPPCGLGLGLGLGLCGKQ**W**
myr-eNOS	myr-GNLKSVGQEPGPPCGLGLGLGLGLCGKQ**W**
eNOS-pal	GNLKSVGQEPGPPC(pal)GLGLGLGLGLC(pal)GKQ**W**
myr-eNOS-pal	myr-GNLKSVGQEPGPPC(pal)GLGLGLGLGLC(pal)GKQ**W**

[a] myr is the myristic acyl chain and pal the palmitic acyl chain. The tryptophan residue added is shown in bold.

Fluorescence Measurements. Fluorescence studies were carried out on a SLM Aminco 8000C spectrofluorimeter, fitted with a 450 W xenon arc and equipped with Glan Thompson polarizers. A 0.2 cm × 1 cm quartz cuvette was used. The buffer used was medium buffer (pH 7.0). The peptide concentration was 3 μM, and the lipid concentration was 0.14 mM. The temperature in the cuvette was maintained by a Polystat Hubber circulating water bath. Excitation was performed at 275 nm, and the emission spectra were recorded over the range from 285 to 450 nm. The contribution of the buffer was always subtracted.

Fluorescence Polarization. Two different probes were employed in the depolarization experiments: 1,6-diphenyl-1,3,5-hexatriene (DPH) and 1-[4-(trimethylammoniumphenyl)-6-phenyl]-1,3,5-hexatriene (TMA-DPH). The former was dissolved in tetrahydrofuran and added to the lipid chloroform solution at a 1:500 molar ratio, and the latter was dissolved in methanol and added to the lipid chloroform solution at a 1:100 molar ratio. The lipid was hydrated in medium buffer at a concentration of 1 mg/mL. The sample was divided into 0.5 mL aliquots, each of them at a lipid concentration of 0.14 mM. DMSO was added to one of these aliquots (control), and peptide from a concentrated DMSO stock solution was added to the others (0.4, 1.4, and 4 μM final concentrations). The samples were measured in 0.2 cm × 1 cm fluorescence cuvettes. The temperature in the cuvette was maintained by a Polystat Hubber circulating water bath. Excitation was performed at 365 nm, and the emission wavelength was 425 nm.

RESULTS

Solid-Phase Synthesis and Acylation of Peptides. Following the methods described in Experimental Procedures, four peptides of 29 amino acids corresponding to the amino-terminal region of eNOS with different degrees of acylation have been obtained: nonacylated peptide (eNOS), myristoylated peptide (myr-eNOS), doubly palmitoylated peptide (eNOS-pal), and dually myristoylated and doubly palmitoylated peptide (myr-eNOS-pal) (Table 1). The Trp residue at the C-terminal position has been added to monitor their interaction with phospholipid vesicles. All peptides were purified by reverse-phase HPLC. eNOS and myr-eNOS were dissolved in a 0.1% TFA/5% acetonitrile mixture and separated with a gradient of acetonitrile. The increased hydrophobicity of eNOS-pal and myr-eNOS-pal made it necessary to dissolve them in a 0.1% TFA/60% ethanol mixture and use a gradient from 5 to 100% propan-2-ol to separate them. All the peptides eluted as single peaks (data not shown). Incorporation of the myristic or palmitic acid into the eNOS sequence considerably increased the elution time. In fact, the presence of two palmitic acids and the additional myristic acid present in myr-eNOS-pal forced the peptide to elute at 100% propan-2-ol. The identity of the peptides was confirmed by amino acid analysis and mass spectrometry. Table 2 shows the molecular mass obtained by mass spectrometry. The experimental data are virtually identical to the values calculated from the amino acid sequence.

Table 2: Molecular Masses of Synthesized Peptides of the N-Terminal Sequence of eNOS

peptide	calcd mass[a] (Da)	*m*/*z* (Da)
eNOS	2836.3	2834.2
myr-eNOS	3046.5	3046.2
eNOS-pal	3312.7	3310.6
myr-eNOS-pal	3522.9	3520.7

[a] The masses of peptides were calculated from the amino acid sequences of peptides and by taking into account the molecular mass of myristic acid (228.21 Da) and palmitic acid (256.24 Da).

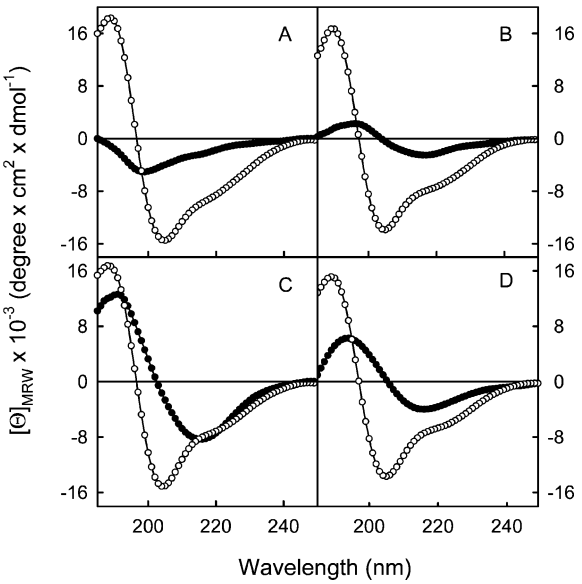

FIGURE 1: Far-UV circular dichroism spectra of eNOS and its acylated peptides alone or in the presence of TFE: (A) eNOS, (B) myr-eNOS, (C) eNOS-pal, and (D) myr-eNOS-pal in (●) 20 mM sodium phosphate (pH 7.0) or (○) 100% TFE. The peptide concentration was 80 μM. These spectra are representative of those obtained for three different preparations.

CD Spectra of Peptides. The conformation of the peptides was determined by circular dichroism. Figure 1 shows the far-UV circular dichroism spectra of nonacylated and acylated peptides in aqueous buffer and in the presence of an organic solvent, TFE. In aqueous solutions, eNOS exhibited a CD spectrum characteristic of a nonordered structure with a minimum centered near 200 nm and a shoulder at 220 nm. However, the acylated peptides showed a shift of the minimum to a higher wavelength, showing spectra with a minimum around 215 nm. Despite the differences in the magnitude of the spectra of acylated peptides, the spectral features are different from those of the nonacylated form and are those of extended structures. The presence of the

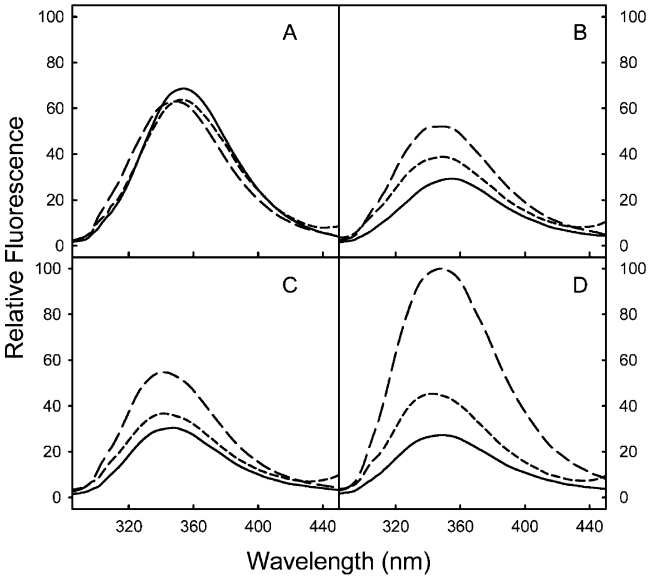

FIGURE 2: Fluorescence emission spectra of eNOS and its acylated peptides in the presence of lipid vesicles: (A) eNOS, (B) myr-eNOS, (C) eNOS-pal, and (D) myr-eNOS-pal in medium buffer (—), PC vesicles (- - -), and PG vesicles (— — —). Emission spectra were obtained upon excitation at 275 nm. The protein concentration was 3 μM, and the lipid concentration was 0.14 mM. The buffer employed was medium buffer (pH 7.0).

nonionic detergent β-D-octyl glucopyranoside up to 20% did not modify the shape of the spectrum of acylated peptides but decreased the ellipticity to values close to those in the presence of phospholipid vesicles (data not shown). The increased population of ordered conformations upon introduction of myristoyl and palmitoyl groups should be the result of the hydrophobic environment provided by the acyl chains. TFE has been used to identify the propensity of a polypeptide sequence to adopt ordered structures. When all four peptides are dissolved in 100% TFE, their spectra exhibited a maximum at 190 nm and two minima at 205 and 220 nm, with molar ellipticity values ranging from -13700 deg cm^2 dmol^{-1} for myr-eNOS-pal to -15500 deg cm^2 dmol^{-1} for eNOS (Figure 1). These are characteristics of peptides adopting an α-helical conformation.

Interaction of the Peptides with Phospholipid Vesicles. To explore the ability of the peptides to interact with model membranes that differ in composition, two different approaches have been used: fluorescence emission spectra of peptides in the presence of lipid vesicles and fluorescence depolarization of two probes embedded in the bilayer to monitor changes in the thermal transition properties of the phospholipids.

The peptides have been designed to contain a tryptophan residue at position 29 which would serve as a fluorescent probe for monitoring the interaction with lipid vesicles. One end of the molecule was chosen because of the minimal induced conformational perturbation and the C-terminal one because the N-terminal Gly had to be myristoylated. The fluorescence emission spectra of eNOS and acylated peptides alone or in the presence of PC and PG vesicles are depicted in Figure 2. The position of the maximum of the emission spectra of the eNOS peptide (354 nm) in medium buffer was indicative of a highly polar environment of the tryptophan residue (*27*). Acylation with myristic acid did not modify the position of the maximum, but palmitate induced a significant decrease (347.5−349 nm). Moreover, the acyl chains caused a decrease in the quantum yield of tryptophan in such a way that in a manner independent of the fatty acid content the fluorescence intensity was reduced to 50% of the original value (Figure 2B−D, solid lines).

When PC vesicles were added to the eNOS peptide, a slight decrease in the fluorescence intensity was observed without modifying the position of the maximum while the presence of PG vesicles also reduced slightly the fluorescence intensity but shifted the position of the maximum of the spectrum of eNOS to a lower wavelength (349 nm) (Figure 2A). The fluorescence properties of acylated peptides were modified upon interaction with neutral and acidic phospholipid vesicles. The Trp residue occupied a more hydrophobic environment as a consequence of the interaction with either phospholipid as evidenced by the blue shift of the fluorescence maximum (from 355−349 to 348−341 nm). On the other hand, the fluorescence intensity increased upon interaction, the increase being much higher in the presence of PG than in the presence of PC. In fact, the fluorescence intensity at the maximum of the spectrum of myr-eNOS-pal in the presence of PG is almost double that of the parent peptide, eNOS. Thus, the fluorescence quenching which appears as a consequence of acylation completely disappears upon interaction with negatively charged phospholipids. This would be indicative of a conformational change which moves the Trp farther from the side chains responsible for the quenching.

The effect of eNOS and acylated peptides on the thermotropic behavior of synthetic phospholipids was assessed by fluorescence depolarization of DPH and its polar derivative, TMA-DPH, incorporated into the bilayer. The peptides were allowed to interact with DMPC and DMPG vesicles for 1 h at 37 °C. The two fluorescent probes were employed in the assays so that the fluidity of both the inner and outer part of the bilayer could be monitored. DPH is assumed to be aligned with the phospholipid acyl chains giving information about the hydrophobic core of the bilayer (*28*, *29*), whereas TMA-DPH has a shallower location due to the anchoring of its nonfluorescent polar moiety to the lipid−water interface and interacts with both the phospholipid polar headgroups and the fatty acyl chain region, probably as far down as C8−C10 (*30*, *31*).

The addition of acylated peptides to DMPG and DMPC vesicles modified the phase transition curves, mainly decreasing the fluidity of the bilayer above the transition temperature. Thus, the amplitude of the phase transition was considerably reduced without significantly affecting the gel-to-liquid crystalline transition temperature. To compare the effect of the peptides on the thermotropic behavior of DMPC and DMPG phospholipids, the changes in the amplitude of the thermal transition (ΔP) at increasing peptide concentrations for DPH- and TMA-DPH-labeled phospholipids were plotted (Figure 3). It can be observed that the eNOS peptide did not produce any effect on the thermal transition of neutral phospholipids that was independent of the probe used or the peptide concentration employed (Figure 3A,C), and only a small decrease in the ΔP value was observed when a concentration of 4 μM was added to DPH-labeled DMPG vesicles, affecting the phospholipid acyl chain in its fluid state. However, the acylated peptides decreased the amplitude of the thermal transition in a concentration-dependent man-

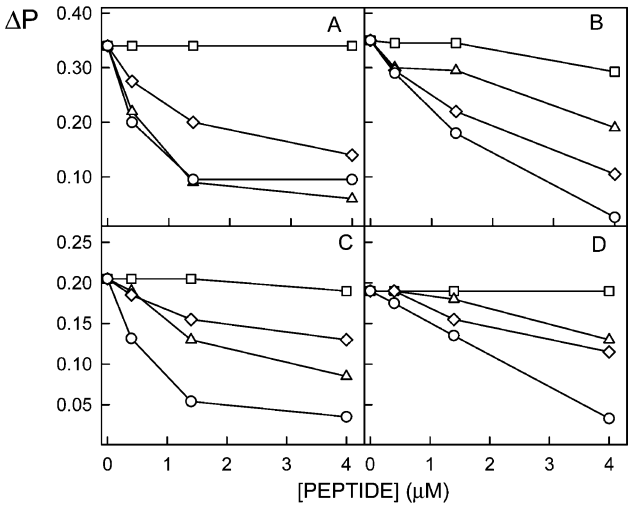

FIGURE 3: Changes in the amplitude of the thermal transition (ΔP) of DPH (A and B)- and TMA-DPH (C and D)-labeled DMPC (A and C) and DMPG (B and D) vesicles with increasing peptide concentrations: (□) eNOS, (△) myr-eNOS, (◇) eNOS-pal, and (○) myr-eNOS-pal. The ΔP value is defined as the difference between the fluorescence polarization values measured at 10 and 45 °C. The phospholipid concentration was 0.14 mM.

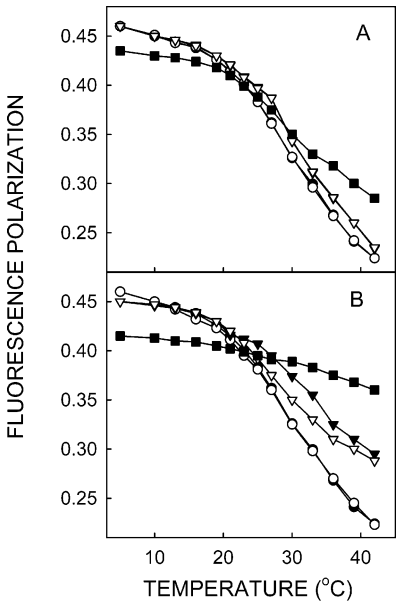

FIGURE 4: Fluorescence polarization of DPH-labeled DMPC/10% Cho/10% SM vesicles: (●) vesicles alone, (○) eNOS, (▼) myr-eNOS, (▽) eNOS-pal, and (■) myr-eNOS-pal. The phospholipid concentration was 0.14 mM, and the peptide concentrations were 0.4 (A) and 1.4 μM (B).

ner. At 4 μM peptide, the transition of DPH-labeled DMPC vesicles is almost completely abolished when myristoylated, palmitoylated, and dually acylated peptides were present (Figure 3A). When acidic vesicles were used, only myr-eNOS-pal canceled the transition at the maximum concentration employed, although the other two peptides also affect the microviscosity above the transition temperature, the effect of eNOS-pal being stronger than that of myr-eNOS. When TMA-DPH was used to monitor shallower domains, similar results were obtained except that only the triacylated peptide was able to cancel the transition and that the myr-eNOS induced more significant changes than eNOS-pal in TMA-DPH-labeled DMPC vesicles (Figure 3C). Control experiments carried out in the presence of equivalent concentrations of the free fatty acid (myristic or palmitic acid) indicated that the observed effects should be due to the amino acid moiety of the acylated peptide since the acyl chain alone did not modify either the order parameter or the transition temperature (data not shown). Then, the presence of any fatty acid allows the peptide to interact with both deep hydrophobic domains of the bilayer and those closer to the polar headgroup.

The effect of the peptides on the thermal transition of more complex vesicles was also studied. Figure 4 shows the fluorescence depolarization profiles of DPH-labeled DMPC vesicles containing 10% cholesterol and 10% sphingomyelin, two lipids present in the lipid composition of caveolae, alone and in the presence of peptide concentrations of 0.14 and 1.4 μM. Although the concentration of cholesterol and sphingomyelin in caveolae is higher than 10% [30% cholesterol and 15−20% sphingomyelin (*32*)], we used that concentration to distinguish the effect of the different peptides on the thermal transition. A higher concentration would abolish the normal sharp thermal transition between gel and liquid crystalline phases. Below the T_m, cholesterol weakens the packing of the headgroup, increasing the fluidity of the ordered gel phase, while above the T_m, the reduction in the degree of freedom of acyl chains causes the membrane to condense with a concomitant decrease in fluidity (*33*). The thermal transition of the vesicles in the absence of peptide is indeed less steep than that of pure DMPC because of the presence of cholesterol [Figure 4 (●)]. At 0.4 μM peptide, only myr-eNOS-pal diminished the transition amplitude, affecting the acyl chain mobility both below and above the transition temperature. At 1.4 μM peptide, the triacylated peptide almost completely canceled the transition whereas myr-eNOS and eNOS-pal reduce the transition amplitude by 30%, affecting only the acyl chains in the fluid state.

CD of Peptide/Phospholipid Mixtures. The CD spectra of the peptides in the presence of lipid vesicles of both acidic and neutral phospholipids are shown in Figure 5. The spectra shown are those obtained at a protein:lipid ratio of 1:10, although a gradual change of the spectrum from the one in the absence of added phospholipid vesicles to the one at that protein:lipid ratio was observed. Increasing the lipid concentration did not modify the spectrum any further. When the peptides were challenged by either DMPG or DMPC vesicles, the CD spectra of the peptides underwent significant conformational changes. The largest change corresponded to the eNOS peptide. From an existing nonordered conformation, the nonacylated peptide adopted an extended conformation, featuring a minimum at 213 nm, in the presence of DMPG. However, the presence of DMPC did not modify the shape of the eNOS peptide spectrum, and only a decrease of the molar ellipticity values was observed (from −5070 deg cm^2 dmol^{-1} at 199 nm to −12200 deg cm^2 dmol^{-1} at 201 nm). This could be due to the fact that the eNOS peptide is aggregated in solution and the presence of neutral phospholipids decreased the amount of such aggregates (*34*) while maintaining the nonordered conformation.

The extended conformation induced by acylation (Figure 1) is modified somehow as a consequence of the interaction with acidic phospholipids. A small shift of the position of the minimum and a decrease in the ellipticity value were observed (Figure 5). The spectra of the three acylated peptides in the presence of DMPG vesicles were similar with

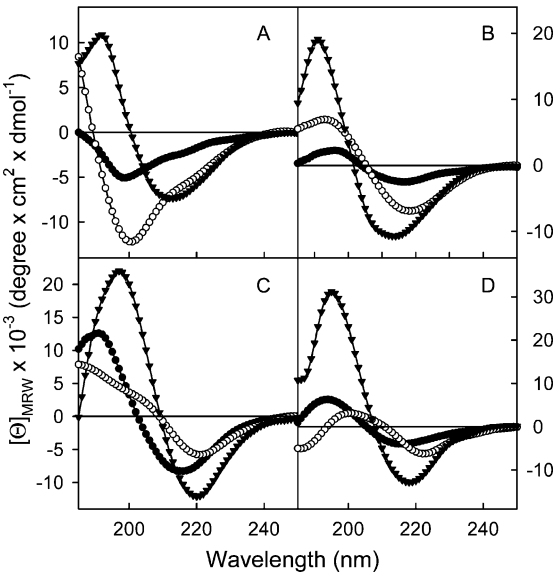

FIGURE 5: Far-UV circular dichroism spectra of eNOS and its acylated peptides in the presence of DMPC or DMPG vesicles: (A) eNOS, (B) myr-eNOS, (C) eNOS-pal, and (D) myr-eNOS-pal with (●) peptide alone, (▼) DMPG vesicles, and (○) DMPC vesicles. The peptide concentration was 80 μM. The peptide:lipid ratio was 1:10. The buffer employed was 20 mM sodium phosphate (pH 7.0). These spectra are representative of these obtained for three different preparations.

a minimum at 214−219 nm and ellipticity values ranging from −10700 deg cm^2 $dmol^{-1}$ for myr-eNOS and −11200 deg cm^2 $dmol^{-1}$ for eNOS-pal to −12800 deg cm^2 $dmol^{-1}$ for myr-eNOS-pal (Figure 5). In the presence of DMPC vesicles, the CD spectra of myristoylated, palmitoylated, or dually acylated peptides exhibited a minimum centered at 218−222 nm and molar ellipticity values ranging from −5800 to −6900 deg cm^2 $dmol^{-1}$ (Figure 5).

DISCUSSION

Covalent attachment of fatty acids to proteins is a common form of protein modification which has been shown to influence both structure and interaction with membranes. To shed some light on the membrane perturbing properties of acylated proteins, we have synthesized a peptide which includes the first 28 amino acids of the N-terminal region of eNOS. Two targeting signals are contained within that eNOS sequence. The Gly residue at the N-terminus end of the protein is irreversibly myristoylated, and the cysteine residues at positions 15 and 26 become reversibly palmitoylated, in a process known to be involved in caveolar translocation. In vivo, the subcellular localization of the 1203-amino acid eNOS is dictated by its N-terminal end. In fact, constructs of the first 35 (*20*) or 55 amino acids (*14*) of eNOS are sufficient to determine a subcellular distribution similar to that of the wild-type protein. We might, therefore, infer that all the information necessary for the subcellular targeting of eNOS might be contained within these first 30 residues. With that in mind, we have analyzed the structural and membrane interacting properties of the isolated N-terminal end of eNOS in different acylation states. From the original eNOS sequence, we have obtained three additional peptides with different degrees of acylation: myristoylated, doubly palmitoylated, and dually myristoylated and doubly palmitoylated peptides. The four peptides are highly pure as demonstrated by HPLC, amino acid analysis, and mass spectrometry.

From a structural point of view, it has been previously shown that palmitoyl groups both increase (*35*) and decrease (*36*) the helical content of pulmonary surfactant protein C. CD spectra of the peptide corresponding to the N-terminal sequence of eNOS show that it exhibits a great conformational flexibility, being able to adopt different secondary structures when challenged by different types of environment. Thus, the eNOS peptide has a nonordered conformation in phosphate buffer. When the peptide is dissolved in TFE, a solvent which can induce stable conformations in peptides which are unstructured in solution (*37*), it adopts mainly a helical conformation. Moreover, acylation itself, either myristic and/or palmitic, confers the peptide the ability to adopt extended conformations, indicated by the fact that the CD spectrum of all acylated peptides has a minimum at ∼215 nm characteristic of β-sheet structure. Although N-terminally truncated eNOS forms have been crystallized and their atomic structures obtained, none of them contains the sequence stretch described in this work. The observation that the myristoylated N-terminal amino acid peptide of eNOS adopts an extended conformation in solution suggests, although it does not confirm, that this extended conformation might be associated with the N-terminal β-sheet lariat observed in the truncated three-dimensional structure obtained from crystallographic data (*38*). Fluorescence properties of the Trp residue indicate that acylation induced some type of conformational change which shields the Trp in a more hydrophobic environment. The formation of the extended conformation could be responsible for such a change, although, as indicated for other acylated polypeptide chains, peptide aggregation or micelle formation could also induce the observed shift (*39*). However, the maintenance of the spectral features in the presence of the detergent β-D-octyl glucopyranoside would indicate that the conformational changes induced upon acylation are not a consequence of the greater degree of self-association of the acylated peptides.

With respect to the role of acylation in the interaction of polypeptide chains with membranes, there are controversial examples in the literature. Thus, it has been shown that the N-terminal segment of pulmonary surfactant lipopeptide SP-C has an intrinsic propensity to interact with phospholipid bilayers in the absence of acylation (*40*). However, palmitoylation of peptides derived from the cysteine-rich domain of SNAP-23 is essential for membrane association (*41*). In several other cases, a lipid moiety represents an additional binding energy necessary to achieve stable interactions (for a review, see ref *42*).

Fluorescence polarization studies show that the polypeptide sequence corresponding to the N-terminal region of eNOS is able to interact with model membranes composed of acidic phospholipids, although the reduction of the transition amplitude is much smaller than that induced by any of the acylated peptides and is observed at only the highest concentration that was assayed. This reduction could be a consequence of the ionic interaction between the polar headgroup of the phospholipid and the amino acid sequence which possesses a net charge of +2. However, the behavior observed for the acylated peptides is that of an integral membrane protein which strongly restricts the mobility of the phospholipid acyl chains, suggesting the insertion of the

peptide into the membrane. At a peptide concentration of 4 μM, myr-eNOS-pal completely abrogated the thermal transition as monitored by fluorescence polarization of the probes DPH and TMA-DPH, which indicates that the peptide interacts both with the hydrophobic portion of the bilayer and with shallower domains, preventing the phospholipid molecules from undergoing the transition characteristic of pure phospholipid species (*43*). Since equivalent amounts of the corresponding free fatty acid had no effect on the thermotropic behavior of the phospholipids, it seems reasonable to conclude that the effects of acylated peptides are due to the insertion of the peptide into the hydrophobic core of the bilayer probably mediated by the interactions between the fatty acid moiety of the peptide and the acyl chains of the phospholipids. The fact that acylated peptides are able to insert into bilayers of both neutral and acidic phospholipids points out that hydrophobic interactions are more important than ionic ones in eliciting the effects observed for these peptides.

The interaction of the peptides with phospholipid vesicles brings about conformational changes as indicated by fluorescence spectroscopy and circular dichroism. The largest change takes place when eNOS interacts with acidic phospholipids since from a nonordered structure in solution the peptide adopts CD spectral features of extended conformations, which, as mentioned before, are not able to insert into the bilayer but are able to interact with the polar headgroups. The changes observed for acylated peptides are greater in magnitude upon interaction with acidic than with neutral phospholipids, although in both cases the spectral features of an extended conformation are maintained. These results could indicate that there exists some tendency of the N-terminus of eNOS to associate with acidic phospholipids. In this sense, negatively charged phospholipids such as phosphatidylserine and phosphatidylglycerol are known to inhibit eNOS activity through its binding to the calmodulin-binding amphipathic helix that interconnects both domains (*44*). Hence, the N-terminal end of eNOS might target the protein to membrane areas enriched in negatively charged phospholipids, where the reported inhibition might exist. When the intracellular calcium levels are increased and binding of calmodulin to eNOS activates the electron transfer and $^{\bullet}$NO synthesis, this inhibitory association with phospholipids might be lost (*44*).

Finally, another role of lipid modification is to promote membrane targeting. It is a general trend that a single lipophilic modification is not sufficient to target a protein to a specific membrane and that two lipid moieties are necessary (*42*). Specifically, myristate and palmitate are necessary and sufficient for the promotion of targeting to rafts (*45*, *46*). In the case of eNOS, it has been shown that palmitoylation takes place in only protein molecules which have been previously myristoylated (*18*−*21*) and that this protein is regulated through a palmitoylation−depalmitoylation cycle. If both types of acylation induce targeting to cholesterol/sphingomyelin-enriched domains, eNOS would be transiently associated with cellular membranes (*47*, *48*).

Of the four peptide species that we describe in this work, only two exist in the corresponding acylated full-length proteins, that is, myr-eNOS and myr-eNOS-palm. According to the circular dichroism data, both of them are able to display very similar secondary structures both in solution and in association with vesicles composed of DMPC or DMPG. However, when interacting with phospholipid vesicles, both of them display a distinct degree of perturbation of the lipid moiety according to our fluorescence spectra and fluorescence depolarization measurements. It is remarkable that in pure DMPC liposomes, the myr-eNOS peptide and the myr-eNOS-pal peptide display similar membrane perturbing properties at 1.4 μM peptide (Figure 3A). Interestingly, when we introduce cholesterol and sphingomyelin at 10% (Figure 4A,B), the perturbation exerted by the triacylated peptide becomes much more profound. However, since the three acylated peptides exerted some degree of perturbation on the thermal transition of these vesicles, no conclusion can be drawn about the possible role of acylation in the translocation to sphingomyelin- and cholesterol-enriched caveolar subdomains.

REFERENCES

1. Resh, M. D. (1999) Fatty acylation of proteins: New insights into membrane targeting of myristoylated and palmitoylated proteins, *Biochim. Biophys. Acta 1451*, 1−16.
2. Gordon, J. I., Duronio, R. J., Rudnick, D. A., Adams, S. P., and Goke, G. W. (1991) Protein N-myristoylation, *J. Biol. Chem. 266*, 8647−8650.
3. Weston, S. A., Camble, R., Colls, J., Rosenbrock, G. M., Taylor, I., Egerton, M., Tucker, A. D., Tunnicliffe, A., Mistry, A., Mancia, T., de la Tortelle, E., Irwin, J., Bricogne, G., and Pauptit, R. A. (1998) Crystal structure of the anti-fungal target N-myristoyl transferase, *Nat. Struct. Biol. 5*, 213−221.
4. Bhatnagar, R. S., Futterer, K., Waksman, G., and Gordon, J. I. (1999) The structure of myristoyl-CoA:protein N-myristoyltransferase, *Biochim. Biophys. Acta 1441*, 162−172.
5. Linder, M. E., and Deschenes, R. J. (2003) New insights into the mechanisms of protein palmitoylation, *Biochemistry 42*, 4311−4320.
6. Dunphy, J. T., and Linder, M. E. (1998) Signalling functions of protein palmitoylation, *Biochim. Biophys. Acta 1436*, 245−261.
7. Lobo, S., Greentree, W. K., Linder, M. E., and Deschenes, R. J. (2002) Identification of a Ras palmitoyltransferase in *Saccharomyces cerevisiae*, *J. Biol. Chem. 277*, 41268−41273.
8. Roth, A. F., Feng, Y., Chen, L., and Davis, N. G. (2002) The yeast DHHC cysteine-rich domain protein Akr1p is a palmitoyl transferase, *J. Cell Biol. 159*, 23−28.
9. Swarthout, J. T., Lobo, S., Farh, L., Croke, M. R., Greentree, W. K., Deschenes, R. J., and Linder, M. E. (2005) DHHC9 and GCP16 constitute a human protein fatty acyltransferase with specificity for H- and N-ras, *J. Biol. Chem. 280*, 31141−31148.
10. Bañó, M. C., Jackson, C. S., and Magee, A. I. (1998) Pseudo-enzymatic S-acylation of a myristoylated yes protein tyrosine kinase peptide in vitro may reflect non-enzymatic S-acylation in vivo, *Biochem. J. 330*, 723−731.
11. Duncan, J. A., and Gilman, A. G. (1996) Autoacylation of G protein α subunits, *J. Biol. Chem. 271*, 23594−23600.
12. Veit, M. (2000) Palmitoylation of the 25-kDa synaptosomal protein (SNAP-25) in vitro occurs in the absence of an enzyme, but is stimulated by binding to syntaxin, *Biochem. J. 345*, 145−151.
13. Bélanger, C., Ansanay, H., Qanbar, R., and Bouvier, M. (2001) Primary sequence requirements for S-acylation of β_2-adrenergic receptor peptides, *FEBS Lett. 499*, 59−64.
14. Navarro-Lérida, I., Álvarez-Barrientos, A., Gavilanes, F., and Rodríguez-Crespo, I. (2002) Distance-dependent cellular palmitoylation of de-novo-designed sequences and their translocation to plasma membrane subdomains, *J. Cell Sci. 115*, 3119−3130.
15. Moncada, S., and Higgs, A. (1993) The L-arginine-nitric oxide pathway, *N. Engl. J. Med. 329*, 2002−2012.
16. Bredt, D. S., and Snyder, S. H. (1994) Nitric oxide. A physiologic messenger molecule, *Annu. Rev. Biochem. 63*, 175−195.
17. Feron, O., Dessy, C., Moniotte, S., Desager, J. P., and Balligand, J. L. (1999) Hypercholesterolemia decreases nitric oxide production by promoting the interaction of caveolin and endothelial nitric oxide synthase, *J. Clin. Invest. 103*, 897−905.

18. Busconi, L., and Michel, T. (1993) Endothelial nitric oxide synthase. N-Terminal myristoylation determines subcellular localization, *J. Biol. Chem. 268*, 8410−8413.
19. Robinson, L. J., Busconi, L., and Michel, T. (1995) Agonist-modulated palmitoylation of endothelial nitric oxide synthase, *J. Biol. Chem. 270*, 995−998.
20. Liu, J., Hughes, T. E., and Sessa, W. C. (1997) The first 35 amino acids and fatty acylation sites determine the molecular targeting of endothelial nitric oxide synthase into the Golgi region of cells: A green fluorescent protein study, *J. Cell Biol. 137*, 1525−1535.
21. Sessa, W. C., García-Cardeña, G., Liu, J., Keh, A., Pollock, J. S., Bradley, J., Thiru, S., Braverman, I. M., and Desai, K. M. (1995) The Golgi association of endothelial nitric oxide synthase is necessary for the efficient synthesis of nitric oxide, *J. Biol. Chem. 270*, 17641−17644.
22. Sakoda, T., Hirata, K., Kuroda, R., Miki, N., Suematsu, M., Kawashima, S., and Yokoyama, M. (1995) Myristoylation of endothelial cell nitric oxide synthase is important for extracellular release of nitric oxide, *Mol. Cell. Biochem. 152*, 143−148.
23. García-Cardeña, G., Oh, P., Liu, J., Schnitzer, J. E., and Sessa, W. C. (1996) Targeting of nitric oxide synthase to endothelial cell caveolae via palmitoylation: Implications for nitric oxide signaling, *Proc. Natl. Acad. Sci. U.S.A. 93*, 6448−6453.
24. Michel, J. B., Feron, O., Sacks, D., and Michel, T. (1997) Caveolin versus calmodulin. Counterbalancing allosteric modulators of endothelial nitric oxide synthase, *J. Biol. Chem. 272*, 15583−15586.
25. King, D. S., Fields, C. G., and Fields, G. B. (1990) A cleavage method which minimizes side reactions following Fmoc solid-phase peptide synthesis, *Int. J. Pept. Protein Res. 36*, 255−266.
26. Beekman, N. J. C. M., Schaaper, W. M. M., Tesser, G. I., Dalsgaard, K., Kamstrup, S., Langeveld, J. P. M., Boshuizen, R. S., and Meloen, R. H. (1997) Synthetic peptide vaccines: Palmitoylation of peptide antigens by a thioester bond increases immunogenicity, *J. Pept. Res. 50*, 357−364.
27. Eftink, M. R. (1991) Fluorescence techniques for studying protein structure, *Methods Biochem. Anal. 35*, 127−205.
28. Lentz, B. R., Barenholz, Y., and Thompson, T. E. (1976) Fluorescence depolarization studies of phase transitions and fluidity in phospholipid bilayers. 2. Two-component phosphatidylcholine liposomes, *Biochemistry 15*, 4529−4537.
29. Andrich, M. P., and Vanderkooi, J. M. (1976) Temperature dependence of 1,6-diphenyl-1,3,5-hexatriene fluorescence in phospholipid artificial membranes, *Biochemistry 15*, 1257−1261.
30. Prendergast, F. G., Haugland, P. J., and Callahan, P. J. (1981) 1-[4-(Trimethylamino)phenyl]-6-phenylhexa-1,3,5-triene: Synthesis, fluorescence properties, and use as a fluorescence probe of lipid bilayers, *Biochemistry 20*, 7333−7338.
31. Kaiser, R. D., and London, E. (1998) Location of diphenylhexatriene (DPH) and its derivatives within membranes: Comparison of different fluorescence quenching analyses of membrane depth, *Biochemistry 37*, 8180−8190.
32. London, E. (2002) Insights into lipid raft strtucture and formation from experiments in model membranes, *Curr. Opin. Struct. Biol. 12*, 480−486.
33. Brown, D. A., and London, E. (1998) Structure and origin of ordered lipid domains in biological membranes, *J. Membr. Biol. 164*, 103−114.
34. Laczko, I., Hollosi, M., Vass, E., and Toth, G. K. (1998) Liposome-induced conformational changes of an epitopic peptide and its palmitoylated derivative of influenza virus hemagglutinin, *Biochem. Biophys. Res. Commun. 249*, 213−217.
35. Szyperski, T., Vandenbussche, G., Curstedt, T., Ruysschaert, J. M., Wuthrich, K., and Johansson, J. (1998) Pulmonary surfactant-associated polypeptide C in a mixed organic solvent transforms from a monomeric α-helical state into insoluble *β*-sheet aggregates, *Protein Sci. 7*, 2533−2540.
36. Creuwels, L. A., Demel, R. A., van Golde, L. M., Benson, B. J., and Haagsman, H. P. (1993) Effect of acylation on structure and function of surfactant protein C at the air−liquid interface, *J. Biol. Chem. 268*, 26752−26758.
37. Yamamoto, Y., Ohkubo, T., Kohara, A., Tanaka, T., and Kikuchi, M. (1990) Conformational requirement of signal sequences functioning in yeast: Circular dichroism and ^{1}H nuclear magnetic resonance studies of synthetic peptides, *Biochemistry 29*, 8998−9006.
38. Raman, C. S., Li, H., Martasek, P., Kral, V., Masters, B. S., and Poulos, T. L. (1998) Crystal structure of constitutive endothelial nitric oxide synthase: A paradigm for pterin function involving a novel metal center, *Cell 95*, 939−950.
39. Harishchandran, A., and Nagaraj, R. (2005) Interaction of a pseudosubstrate of protein kinase C and its myristoylated form with lipid vesicles: Only the myristoylated form translocates into the lipid bilayer, *Biochim. Biophys. Acta 1713*, 73−82.
40. Plasencia, I., Rivas, L., Keough, K. M. W., Marsh, D., and Perez-Gil, J. (2004) The N-terminal segment of pulmonary surfactant lipopeptide SP-C has intrinsic propensity to interact with and perturb phospholipid bilayers, *Biochem. J. 377*, 183−193.
41. Pallavi, B., and Nagaraj, R. (2003) Palmitoylated peptides from the cysteine-rich domain of SNAP-23 cause membrane fusion depending on peptide length, position of cysteines, and extent of palmitoylation, *J. Biol. Chem. 278*, 12737−12744.
42. Resh, M. D. (2004) Membrane targeting of lipid modified signal transduction proteins, in *Subcellular Biochemistry* (Quinn, P. J., Ed.) Vol. 37, pp 217−232, Kluwer Academic/Plenum Publishers, New York.
43. Papahadjopoulos, D., Moscarello, M., Eylar, E. H., and Isac, T. (1975) Effects of proteins on thermotropic phase transitions of phospholipid membranes, *Biochim. Biophys. Acta 401*, 317−335.
44. Venema, R. C., Sayegh, H. S., Arnal, J. F., and Harrison, D. G. (1995) Role of the enzyme calmodulin-binding domain in membrane association and phospholipid inhibition of endothelial nitric oxide synthase, *J. Biol. Chem. 270*, 14705−14711.
45. Galbiati, F., Volonte, D., Meani, D., Milligan, G., Lublin, D. M., Lisanti, M. P., and Parenti, M. (1999) The dually acylated NH_2-terminal domain of gi1α is sufficient to target a green fluorescent protein reporter to caveolin-enriched plasma membrane domains. Palmitoylation of caveolin-1 is required for the recognition of dually acylated g-protein α subunits in vivo, *J. Biol. Chem. 274*, 5843−5850.
46. Zacharias, D. A., Violin, J. D., Newton, A. C., and Tsien, R. Y. (2002) Partitioning of lipid-modified monomeric GFPs into membrane microdomains of live cells, *Science 296*, 913−916.
47. McCabe, J. B., and Berthiaume, L. G. (1999) Functional roles for fatty acylated amino-terminal domains in subcellular localization, *Mol. Biol. Cell 10*, 3771−3786.
48. Simons, K., and Toomre, D. (2000) Lipid rafts and signal transduction, *Nat. Rev. Mol. Cell Biol. 1*, 31−39.

BI0514865